Available online at www.sciencedirect.com
SCIENCE DIRECT®
Electrochemistry Communications 8 (2006) 329–335
electrochemistry communications
www.elsevier.com/locate/elecom

Safety characteristics of $Li(Ni_{0.8}Co_{0.15}Al_{0.05})O_2$ and $Li(Ni_{1/3}Co_{1/3}Mn_{1/3})O_2$

Ilias Belharouak, Wenquan Lu, Donald Vissers, Khalil Amine *

Chemical Engineering Division, Argonne National Laboratory, Electrochemical Technology Program, 9700 South Cass Avenue, Argonne, IL 60439, USA

Received 3 November 2005; received in revised form 5 December 2005; accepted 9 December 2005
Available online 18 January 2006

Abstract

Layered $Li_{0.45}(Ni_{0.8}Co_{0.15}Al_{0.05})O_2$ and $Li_{0.55}(Ni_{1/3}Co_{1/3}Mn_{1/3})O_2$ materials have been, respectively, prepared by a chemical delithiation of layered $Li(Ni_{0.8}Co_{0.15}Al_{0.05})O_2$ and $Li(Ni_{1/3}Co_{1/3}Mn_{1/3})O_2$ compounds using NO_2BF_4 oxidizer in an acetonitrile medium. The thermal gravimetric results show that both $Li_{0.45}(Ni_{0.8}Co_{0.15}Al_{0.05})O_2$ and $Li_{0.55}(Ni_{1/3}Co_{1/3}Mn_{1/3})O_2$ powders release oxygen starting from 190 and 250 °C with an overall oxygen loss of 11 and 9 wt% at 900 °C, respectively. The results show that the oxygen release from these delithiated powders was associated with the occurrence of several structural transformations, ranging from a $R\bar{3}m \rightarrow Fd3m$ (layered → spinel) transition to a $Fd3m \rightarrow Fm3m$ (spinel → NiO-type) transition. The 3 wt% weight gain, solely observed for $Li_{0.55}(Ni_{1/3}Co_{1/3}Mn_{1/3})O_2$ between 800 °C and room temperature, involved a reversible $Fd3m \leftrightarrows Fm3m$ (spinel⇆NiO-type) structural transition. The reactivity of these delithiated powders with electrolytes was investigated by a differential scanning calorimetry (DSC) between room temperature and 375 °C. In the case of $Li_{0.55}(Ni_{1/3}Co_{1/3}Mn_{1/3})O_2$ powder, the DSC result shows that the oxidation of the electrolyte was delayed by 50 °C toward high temperatures with the generation of lower heat when compared to $Li_{0.45}(Ni_{0.8}Co_{0.15}Al_{0.05})O_2$ powder. The relationship between the safety characteristics of $Li_{0.45}(Ni_{0.8}Co_{0.15}Al_{0.05})O_2$ and $Li_{0.55}(Ni_{1/3}Co_{1/3}Mn_{1/3})O_2$ powders and their thermal stability was discussed in the light of their structural rearrangement during the thermal heating processes.
© 2005 Elsevier B.V. All rights reserved.

Keywords: Lithium-ion batteries; Cathode; Thermal stability; High power; HEV

1. Introduction

The US auto industry is in search for high-power lithium-ion batteries that are inexpensive, have excellent calendar life, and better thermal abuse tolerance, to replace the nickel metal hydride batteries currently being used in HEV applications. For this purpose, the Advanced Technology Development (ATD) program was initiated by DOE to help expedite the development of high-power lithium-ion batteries for hybrid electric vehicles (HEVs) under the DOE FreedomCAR Partnership. Under this project, the $Li(Ni_{0.8}Co_{0.15}Al_{0.05})O_2$/graphite cells were extensively studied as a potential cell chemistry for HEV applications, with a primary goal of understanding the power fade mechanisms of these cells [1–3]. A second goal of this project was to conduct detailed thermal abuse studies on selected cell chemistries as well as their battery components [4]. Extensive work carried out on the $Li(Ni_{0.8}Co_{0.15}Al_{0.05})O_2$/graphite cell systems has confirmed that the impedance rise at the cathode is the main cause of the poor calendar life of this system [5,6]. This is because the reactivity in this system involves the reduction of the highly oxidizing and unstable Ni^{4+} that is generated during the charge. When the Ni^{4+} is reduced, it forms an interfacial NiO-type resistive film at the surface of the cathode that leads to the cell power fade [7]. Therefore, there was a need to search for new low-nickel content cathodes that could replace $Li(Ni_{0.8}Co_{0.15}Al_{0.05})O_2$. To this end, $Li(Ni_{1/3}Co_{1/3}Mn_{1/3})O_2$ material was found to meet the hybrid pulse power characteristics (HPPC) requirements for the HEV applications [8]. Our comparative safety study also showed that the

* Corresponding author. Tel.: +1 630 252 3838; fax: +1 630 252 4176.
E-mail address: amine@cmt.anl.gov (K. Amine).

1388-2481/$ - see front matter © 2005 Elsevier B.V. All rights reserved.
doi:10.1016/j.elecom.2005.12.007

$Li(Ni_{1/3}Co_{1/3}Mn_{1/3})O_2$ electrode has much better safety characteristics than the $Li(Ni_{0.8}Co_{0.15}Al_{0.05})O_2$ electrode [8]. This result was particularly important toward enabling the use of lithium-ion batteries in large-scale applications such as HEV. To corroborate this finding, there was a need to understand first the safety characteristics of $Li(Ni_{0.8}Co_{0.15}Al_{0.05})O_2$ and $Li(Ni_{1/3}Co_{1/3}Mn_{1/3})O_2$ powders alone without the interference from other electrode components such as carbon and binder additives.

The present paper reports on the thermal and structural stability of $Li(Ni_{0.8}Co_{0.15}Al_{0.05})O_2$ and $Li(Ni_{1/3}Co_{1/3}Mn_{1/3})O_2$ powders after being subjected to a chemical delithiation using the NO_2BF_4 oxidizer. The thermal degradation of the obtained $Li_{0.45}(Ni_{0.8}Co_{0.15}Al_{0.05})O_2$ and $Li_{0.55}(Ni_{1/3}Co_{1/3}Mn_{1/3})O_2$ oxides was studied using a thermal gravimetric analysis (TGA) combined with an X-ray diffraction (XRD) analysis. The positive active powder/electrolyte reactivity was also investigated by a differential scanning calorimetry (DSC) or accelerated rate calorimetry (ARC) in order to correlate the oxidation of the electrolytes with the oxygen loss released from the oxidized powders at elevated temperatures. Afterwards, the general safety characteristics of $Li_{0.45}(Ni_{0.8}Co_{0.15}Al_{0.05})O_2$ and $Li_{0.55}(Ni_{1/3}Co_{1/3}Mn_{1/3})O_2$ powders were discussed based on the correlation between the oxygen release and the structural transformation during the heat treatment of these active materials.

2. Experimental

$Li(Ni_{0.8}Co_{0.15}Al_{0.05})O_2$ and $Li(Ni_{1/3}Co_{1/3}Mn_{1/3})O_2$ materials were synthesized using metal hydroxide precursors according to a preparation procedure previously reported by Shaju et al. [9]. The chemical delithiation [10,11] of the obtained LiM_TO_2 ($M_T = Ni_{0.8}Co_{0.15}Al_{0.05}$ or $Ni_{1/3}Co_{1/3}Mn_{1/3}$) materials was achieved by stirring the powders in acetonitrile solutions containing NO_2BF_4 oxidizer (molar ratio $LiM_TO_2/NO_2BF_4 = 1$). After 24 h of lithium extraction at room temperature, the solutions were filtered and the remaining powders were washed with acetonitrile several times. The resulting materials were then dried at 80 °C under vacuum for 24 h and thereafter were stored inside an Argon-filled glove box. The inductively coupled plasma (ICP) analysis results revealed that after delithiation of $Li(Ni_{0.8}Co_{0.15}Al_{0.05})O_2$ and $Li(Ni_{1/3}Co_{1/3}Mn_{1/3})O_2$, $Li_{0.45}(Ni_{0.8}Co_{0.15}Al_{0.05})O_2$ and $Li_{0.55}(Ni_{1/3}Co_{1/3}Mn_{1/3})O_2$ were obtained, respectively.

Powder X-ray diffraction (XRD) patterns of the samples were recorded on a Siemens D5000 powder diffractometer using Cu Kα radiation in the angular range of 10–80° (2θ) with a 0.02° (2θ) step. The structural parameters were calculated using a Rietveld profile matching refinement method of the XRD diagrams [12].

Thermal gravimetric analysis (TGA) experiments under a purified air flow were conducted on 30 mg of the chemically delithiated $Li_{0.45}(Ni_{0.8}Co_{0.15}Al_{0.05})O_2$ and $Li_{0.55}(Ni_{1/3}Co_{1/3}Mn_{1/3})O_2$ powders that were placed inside platinum pans, where the reference pan of the furnace, consisted of an empty platinum pan. The data were collected using a Seiko Exstar 6000 instrument at a scan rate of 5 °C/min in the temperature range of 25–920 °C.

Differential scanning calorimetry (DSC) experiments were conducted on the chemically delithiated powders using a Perkin–Elmer Pyris 1 instrument. Typically, 3 mg of $Li_{0.45}(Ni_{0.8}Co_{0.15}Al_{0.05})O_2$ or $Li_{0.55}(Ni_{1/3}Co_{1/3}Mn_{1/3})O_2$ powders and 3 μl of electrolyte were hermetically sealed inside stainless steel high pressure capsules to prevent a leakage of the pressurized solvents. The DSC curves were recorded between room temperature and 375 °C at a scan rate of 10 °C/min. An empty stainless steel capsule was used as a reference pan. To ensure reproducibility, at lease two measurements were conducted for each data point.

3. Results and discussion

Fig. 1 shows the XRD patterns of the $Li(Ni_{0.8}Co_{0.15}Al_{0.05})O_2$ and $Li(Ni_{1/3}Co_{1/3}Mn_{1/3})O_2$ pristine powders and their chemically delithiated phases $Li_{0.45}(Ni_{0.8}Co_{0.15}Al_{0.05})O_2$ and $Li_{0.55}(Ni_{1/3}Co_{1/3}Mn_{1/3})O_2$. In all cases, the observed diffraction lines can be indexed based on the $R\bar{3}m$ space group and are consistent with the layered structure of α-$NaFeO_2$. The delithiated phases have the following hexagonal lattice parameters: $a_h = 2.830$ Å, $c_h = 14.432$ Å for $Li_{0.45}(Ni_{0.8}Co_{0.15}Al_{0.05})O_2$ and $a_h = 2.829$ Å, $c_h = 14.444$ Å for $Li_{0.55}(Ni_{1/3}Co_{1/3}Mn_{1/3})O_2$. In both cases, an expansion of the c parameter was observed when compared to the initial fully lithiated phases, which have hexagonal unit cell parameters of $a_h = 2.862$ Å, $c_h = 14.171$ Å for $Li(Ni_{0.8}Co_{0.15}Al_{0.05})O_2$; and $a_h = 2.860$ Å, $c_h = 14.244$ Å for $Li(Ni_{1/3}Co_{1/3}Mn_{1/3})O_2$.

To initiate the study of their reactivity with electrolytes, DSC curves were first recorded on the chemically delithiated $Li_{0.45}(Ni_{0.8}Co_{0.15}Al_{0.05})O_2$ and $Li_{0.55}(Ni_{1/3}Co_{1/3}Mn_{1/3})O_2$ powders without electrolyte (Fig. 2). In this case, no exothermic reactions were observed. Thereafter, DSC measurements were recorded on $Li_{0.45}(Ni_{0.8}Co_{0.15}Al_{0.05})O_2$ or $Li_{0.55}(Ni_{1/3}Co_{1/3}Mn_{1/3})O_2$ powders in the presence of several electrolytes, e.g., 1.2 M $LiPF_6$/EC:EMC (3:7 wt%). The total heats associated with the observed exothermic peaks are presented in Fig. 2. For $Li_{0.45}(Ni_{0.8}Co_{0.15}Al_{0.05})O_2$/electrolyte combination, the main reaction with the electrolyte occurred around 250 °C with an onset temperature at around 200 °C. However, the reaction for $Li_{0.55}(Ni_{1/3}Co_{1/3}Mn_{1/3})O_2$ powder started at around 260 °C with a predominant exothermic peak observed a little beyond 300 °C (Fig. 2). These DSC data were valuable toward making the following remarks: (i) in the absence of electrolytes, both $Li_{0.45}(Ni_{0.8}Co_{0.15}Al_{0.05})O_2$ and $Li_{0.55}(Ni_{1/3}Co_{1/3}Mn_{1/3})O_2$ powders do not generate heat although they may have decomposed at elevated temperatures; (ii) in the presence of an electrolyte, both $Li_{0.45}(Ni_{0.8}Co_{0.15}Al_{0.05})O_2$ and $Li_{0.55}(Ni_{1/3}Co_{1/3}Mn_{1/3})O_2$ generate exothermic reactions, but the later has a higher onset temperature and a lower heat. To understand the difference in

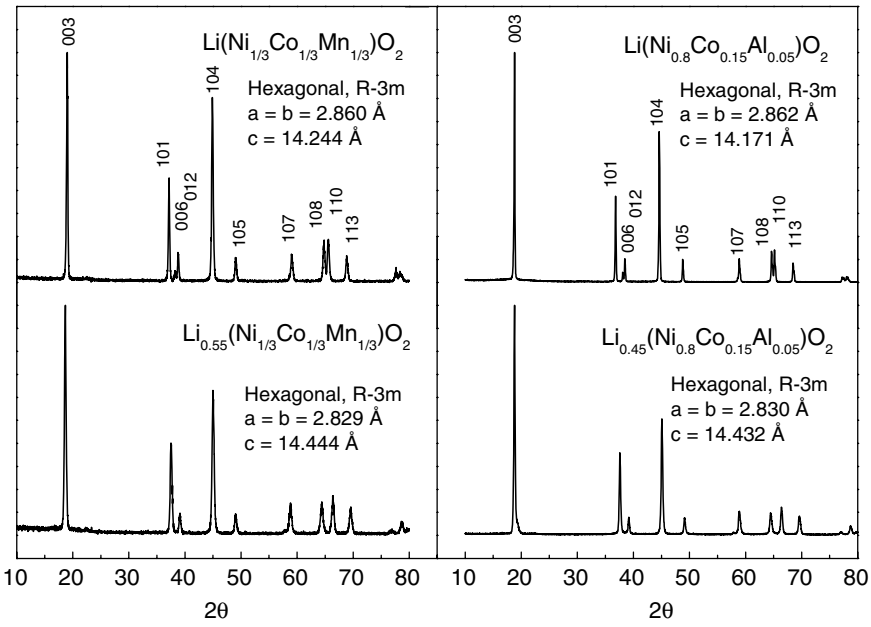

Fig. 1. XRD patterns of pristine $Li(Ni_{0.8}Co_{0.15}Al_{0.05})O_2$ and $Li(Ni_{1/3}Co_{1/3}Mn_{1/3})O_2$ materials and their $Li_{0.45}(Ni_{0.8}Co_{0.15}Al_{0.05})O_2$ and $Li_{0.55}(Ni_{1/3}Co_{1/3}Mn_{1/3})O_2$ deintercalated forms, respectively.

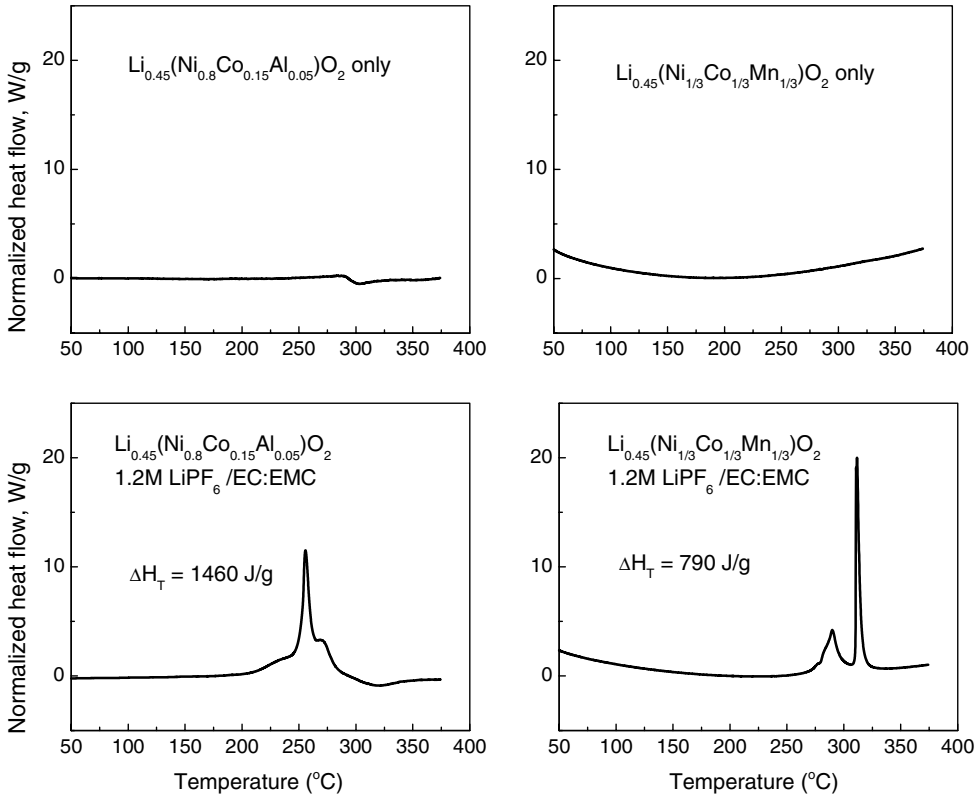

Fig. 2. DSC profiles of $Li_{0.45}(Ni_{0.8}Co_{0.15}Al_{0.05})O_2$ and $Li_{0.55}(Ni_{1/3}Co_{1/3}Mn_{1/3})O_2$ powders in the presence of the 1.2 M $LiPF_6$/EC:EMC (3:7 wt%) electrolyte.

the safety characteristics between these two materials, we investigated the oxygen release from the chemically delithiated $Li_{0.45}(Ni_{0.8}Co_{0.15}Al_{0.05})O_2$ and $Li_{0.55}(Ni_{1/3}Co_{1/3}Mn_{1/3})O_2$ phases by a thermal gravimetric analysis (TGA) and correlated their thermal behavior to their structural transformation during the heating process.

Fig. 3 shows the TGA curve of $Li_{0.45}(Ni_{0.8}Co_{0.15}Al_{0.05})O_2$ recorded between room temperature and

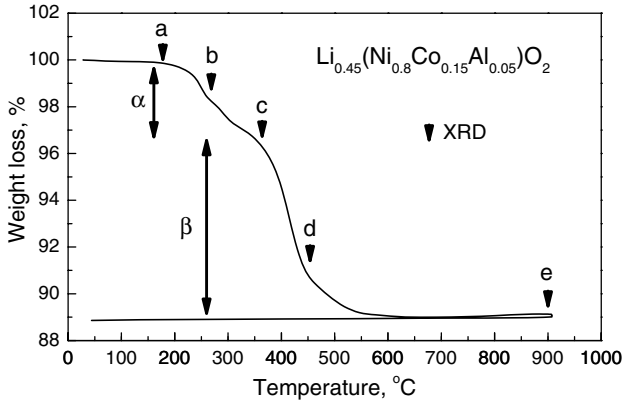

Fig. 3. Thermal gravimetric analysis (TGA), conducted under purified air atmosphere, of the $Li_{0.45}(Ni_{0.8}Co_{0.15}Al_{0.05})O_2$ delithiated cathode.

900 °C under a purified air atmosphere. The thermal degradation of this chemically deintercalated powder occurred in two steps (α and β) with a total weight loss of 11 wt%. The structural stability of $Li_{0.45}(Ni_{0.8}Co_{0.15}Al_{0.05})O_2$ was then studied by XRD (Fig. 4) on samples subjected to different temperatures during the TGA study (Fig. 3). At 175 °C, only a very slight change of the hexagonal cell parameters can be observed. However, at around 265 °C where barely 2 wt% oxygen loss occurred, we noticed that the diffraction lines (1 0 8) and (1 1 0) merged together into a single (0 4 4) diffraction line (65.84° (2θ)) which indicates the formation of a spinel (S.G. Fd3m) phase. In addition, the integrated intensity ratio of $I(0\,0\,3)/I(1\,0\,4)$ peaks became inferior to one. These two observations let us conclude that the phase formed at 265 °C did not ideally fit the description of a disordered α-$NaFeO_2$ ($R\bar{3}m$) or a spinel (Fd3m) phase. Therefore, we believe that at around 265 °C, the lithium atoms start to migrate from their octahedral sites to the adjacent tetrahedral vacant sites with a possibility of a migration of Ni^{2+} to the available Li octahedral sites. These two structural rearrangements could explain both the spinel and disordered character of the resulting phase. At 360 °C, the 4 wt% O_2 loss observed by TGA has led to the formation of a spinel phase (S.G. Fd3m) probably because of the active migration of more Li atoms to the neighboring tetrahedral sites. This assignment was supported by the appearance of the (0 2 2) diffraction line at 31.44° (2θ) which is very specific to a spinel phase (Fd3m, $a = 8.156$ Å) and cannot be attributed to a disordered ($R\bar{3}m$) phase. However, the unusual broadening observed for all the diffraction peaks is still unexplained. A similar phase transition ($R\bar{3}m \rightarrow Fd3m$) was reported by Guilmard et al. in their thermal study of high-nickel concentration based cathodes [13,14]. At 450 °C where 9.2 wt% O_2 is lost from the material, the (0 2 2) diffraction line of the spinel phase disappeared and the resulting phase apparently had more disordered α-$NaFeO_2$ ($R\bar{3}m$) structural character than a spinel (Fd3m) one. At elevated temperatures, the structural change process implies the migration of the Li atoms from their tetrahedra to statistically share the octahedra occupied by Ni, Co and Al atoms. At the end of the TGA experiment (900 °C), a clear structural transition to a NiO-type phase (Fm3m, $a = 4.118$ Å) was observed after the 11 wt% oxygen weight loss from the material. The obtained rock-salt phase indicates that all cations were randomly distributed in the octahedral sites within the oxygenated face centered cubic (fcc) unit cell.

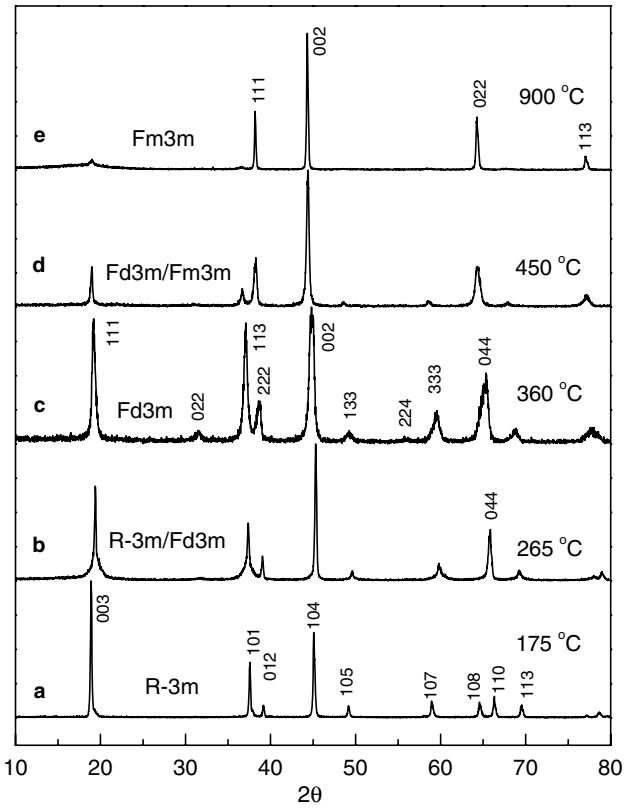

Fig. 4. Evolution of the (XRD) patterns recorded at room temperature on $Li_{0.45}(Ni_{0.8}Co_{0.15}Al_{0.05})O_2$ samples that were subjected to TGA experiments (see Fig. 3).

Fig. 5 shows the TGA curve resulting from the thermal decomposition of $Li_{0.55}(Ni_{1/3}Co_{1/3}Mn_{1/3})O_2$ material. In this case, the total weight loss occurred in three steps (α,

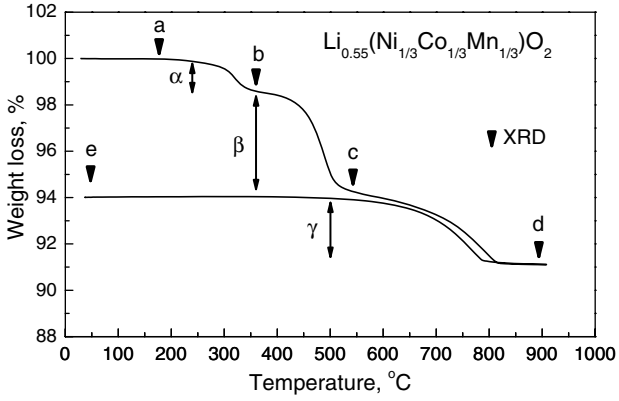

Fig. 5. TGA curve (under purified air) of $Li_{0.55}(Ni_{1/3}Co_{1/3}Mn_{1/3})O_2$ material.

β and γ) between 280 and 820 °C. The steps (α) [280–380 °C] and (β) [380–600 °C] observed for $Li_{0.55}(Ni_{1/3}Co_{1/3}Mn_{1/3})O_2$ presented some similarities when compared to the steps (α) [200–300 °C] and (β) [300–600 °C] observed for $Li_{0.45}(Ni_{0.8}Co_{0.15}Al_{0.05})O_2$ (Fig. 3). However, the starting thermal degradation temperature shifted in the case of $Li_{0.55}(Ni_{1/3}Co_{1/3}Mn_{1/3})O_2$ from around 200 °C (for $Li_{0.45}(Ni_{0.8}Co_{0.15}Al_{0.05})O_2$) to 260 °C, which indicates that the oxygen release from the charged $Li_{0.55}(Ni_{1/3}Co_{1/3}Mn_{1/3})O_2$ cathode can only occur beyond this temperature (260 °C) (Fig. 5). It should be noted that beyond 600 °C, $Li_{0.45}(Ni_{0.8}Co_{0.15}Al_{0.05})O_2$ is completely decomposed, while $Li_{0.55}(Ni_{1/3}Co_{1/3}Mn_{1/3})O_2$ exhibits an additional 3 wt% O_2 loss between 600 and 820 °C (step γ). This result clearly indicates that $Li_{0.55}(Ni_{1/3}Co_{1/3}Mn_{1/3})O_2$ is more stable thermodynamically than $Li_{0.45}(Ni_{0.8}Co_{0.15}Al_{0.05})O_2$. The 3 wt% O_2 loss was fully recovered between 910 and 600 °C during the cooling process, and the resulting material was quite stable thereafter.

To compare the structural stability of $Li_{0.55}(Ni_{1/3}Co_{1/3}Mn_{1/3})O_2$ powder vs. $Li_{0.45}(Ni_{0.8}Co_{0.15}Al_{0.05})O_2$ powder, a room temperature ex-situ XRD study was performed on several $Li_{0.55}(Ni_{1/3}Co_{1/3}Mn_{1/3})O_2$ samples recovered at different temperatures after the TG analysis as shown in Fig. 5. At 175 °C and because of no weight loss, the $Li_{0.55}(Ni_{1/3}Co_{1/3}Mn_{1/3})O_2$ powder did not show any noticeable structural change, i.e., unit cell parameters and diffraction line intensities were similar to those observed before the heat treatment. However, at 360 °C, the 2.5 wt% loss resulted in two majors structural modifications: (a) the (1 0 8) and (1 1 0) diffraction lines shifted toward each other but did not completely merge, and (b) the integrated intensity ratio of $I(0\,0\,3)/I(1\,0\,4)$ peaks became dramatically inferior to one. At this stage, we believe that in spite of the change in the XRD diagram (Fig. 6), the obtained material after treatment at 360 °C had a disordered α-$NaFeO_2$ ($R\bar{3}m$) type structure. The degree of this disorder can be associated with the effectiveness of the Li and metal transition (Co, Ni and Mn) atoms migration to their mutual crystallographic sites. At 540 °C where 5.8 wt% O_2 loss occurred, the material converted to a spinel-type phase (Fd3m). This structural transition was confirmed by both the merger of the (1 0 8) and (1 1 0) diffraction lines into the (0 0 4) line at 65.16° (2θ) and the appearance of the (0 0 2) line at 31.38° (2θ); these two facts are very specific to a spinel (Fd3m) atomic arrangement although the intensity ratio $I(1\,1\,1)/I(0\,0\,4)$ remained inferior to one. At the end of the TGA experiment and after recovering the 3 wt% O_2 loss, the obtained material was indexed based on a spinel (Fd3m, $a = 8.146$ Å) structural model.

To investigate the origin of the O_2 gain in Fig. 5, it was necessary to thermally quench the $Li_{0.55}(Ni_{1/3}Co_{1/3}Mn_{1/3})O_2$ material heated at 910 °C in order to elucidate its structure. Two samples of $Li_{0.55}(Ni_{1/3}Co_{1/3}Mn_{1/3})O_2$ were then treated for 3 h at 900 °C; one of them was slowly cooled down and the second was rapidly quenched using liquid nitrogen. Fig. 7 shows the room temperature XRD patterns of these two samples after the heat treatment. On one hand, the sample that was subject to a slow cooling had a spinel-type structure (Fd3m) with a cubic cell parameter $a = 8.153$ Å; this result was consistent with the finding in Fig. 6. On the other hand, the sample that was quenched at 900 °C and therefore effectively lost 9 wt% O_2, converted to a NiO-type structure (Fm3m) with a cubic cell parameter $a = 4.16$ Å. In this case, the (Fd3m⇆Fm3m) structural

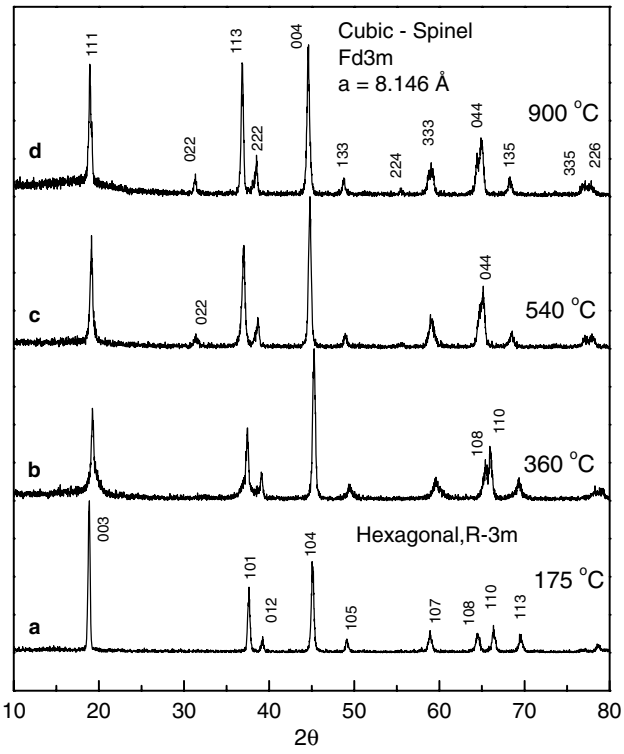

Fig. 6. Room temperature XRD diagrams of $Li_{0.55}(Ni_{1/3}Co_{1/3}Mn_{1/3})O_2$ samples recovered after the TGA experiments (see Fig. 5).

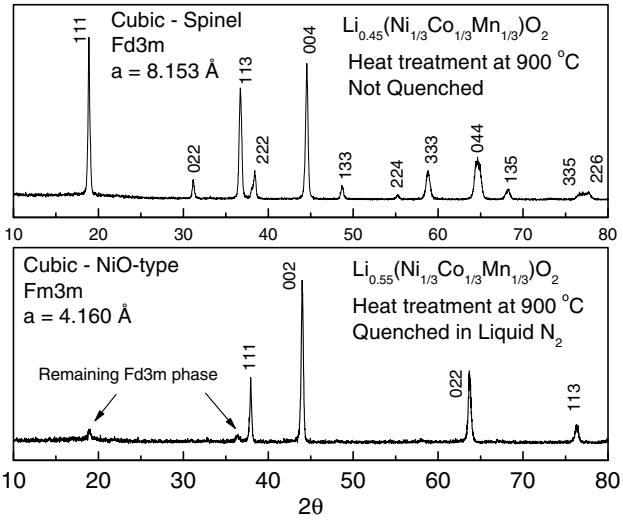

Fig. 7. Comparison between the XRD patterns of $Li_{0.55}(Ni_{1/3}Co_{1/3}Mn_{1/3})O_2$ samples treated at 900 °C for 3 h and followed with and without quenching.

transition was associated with the reversible redox character of Mn^{4+}/Mn^{3+} and Mn^{3+}/Mn^{2+} couples, which at high temperature tend to adopt a lower oxidation state giving rise to a NiO-type phase. The TGA results also show that the 3 wt% O_2 gain, between 810 and 500 °C, was enough to increase the oxidation of manganese to a level that allows the stabilization of a spinel (Fd3m) phase. This transition (Fm3m⇆Fd3m) means that within a similar (fcc) oxygen atomic arrangement, the Li, Ni, Co, and Mn cations can either statistically occupy the same octahedron available for the rock-salt phase ((4a) crystallographic position, Fm3m) or preferably be distributed between the (8a: tetrahedron) and (16d: octahedron) positions of the spinel phase (Fd3m).

From their thermal gravimetric curves, one can conclude that the chemically delithiated $Li_{0.45}(Ni_{0.8}Co_{0.15}Al_{0.05})O_2$ or $Li_{0.55}(Ni_{1/3}Co_{1/3}Mn_{1/3})O_2$ powders have different tendencies to release oxygen. In the case of $Li_{0.55}(Ni_{1/3}Co_{1/3}Mn_{1/3})O_2$, the thermal treatment causes less structural disorder, and therefore the general tendency to release O_2 is slowed down because of the formation of a stable spinel phase during the thermal processes. However, the spinel phase observed in the case of $Li_{0.45}(Ni_{0.8}Co_{0.15}Al_{0.05})O_2$ is thermodynamically unstable, and decomposes by a mechanism that involves more oxygen release from the material to form a NiO-type phase. These structural transitions are not only important from the fundamental point of view, but they are also valuable toward understanding the general safety characteristics of both materials. Indeed, in the zone of reactivity with electrolyte (100–400 °C), the limited structural disorder found for $Li_{0.55}(Ni_{1/3}Co_{1/3}Mn_{1/3})O_2$ was associated with the loss of less than 2 wt% O_2; whereas the 6 wt% O_2 release observed in the case of $Li_{0.45}(Ni_{0.8}Co_{0.15}Al_{0.05})O_2$ was accompanied with a significant structural damage. These results clearly indicate that the $Li(Ni_{1/3}Co_{1/3}Mn_{1/3})O_2$ material has better safety characteristics than the $Li(Ni_{0.8}Co_{0.15}Al_{0.05})O_2$ material.

The reactivity of the Layered $Li_{0.45}(Ni_{0.8}Co_{0.15}Al_{0.05})O_2$ and $Li_{0.55}(Ni_{1/3}Co_{1/3}Mn_{1/3})O_2$ oxide powders with the 1.2 M $LiPF_6$/EC/EMC (3:7 wt%) electrolyte was conducted, using the accelerated rate calorimetry, in sealed stainless containers containing 100 mg of the powder and 100 mg of the electrolyte. The sealed containers were heated between room temperature and 400 °C . After completion of the reaction, the containers were opened and the remaining powders were analyzed by XRD (Fig. 8). The XRD results reveal the presence of a NiO-type phase and LiF after the reaction of both $Li_{0.45}(Ni_{0.8}Co_{0.15}Al_{0.05})O_2$ and $Li_{0.55}(Ni_{1/3}Co_{1/3}Mn_{1/3})O_2$ with the electrolyte. In addition, a metallic nickel phase was observed after the decomposition of $Li_{0.45}(Ni_{0.8}Co_{0.15}Al_{0.05})O_2$, which indicates a further reduction of the NiO-type phase and more oxygen release from this material that reacted with the electrolyte. In the case of $Li_{0.55}(Ni_{1/3}Co_{1/3}Mn_{1/3})O_2$, no metallic nickel was observed. However, two additional phases, $MnCO_3$ and Li_2CO_3, were obtained. These two phases are the result

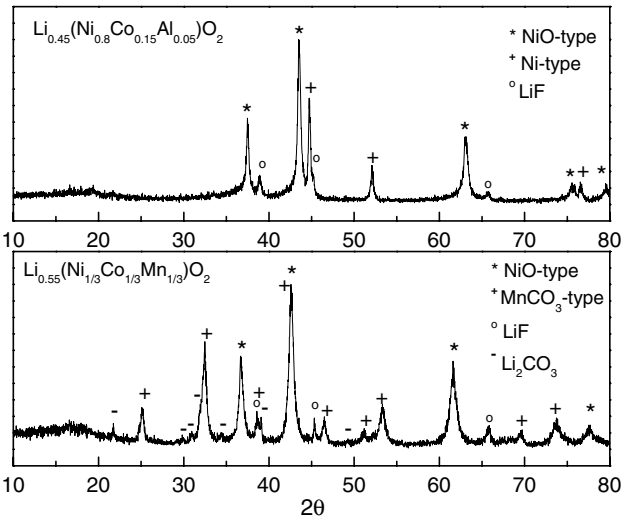

Fig. 8. XRD patterns of samples recovered after the reaction of $Li_{0.45}(Ni_{0.8}Co_{0.15}Al_{0.05})O_2$ and $Li_{0.55}(Ni_{1/3}Co_{1/3}Mn_{1/3})O_2$ with the 1.2 M $LiPF_6$/EC/EMC (3:7 wt%) electrolyte.

of the reaction of manganese and the remaining lithium, from the decomposition of $Li_{0.55}(Ni_{1/3}Co_{1/3}Mn_{1/3})O_2$, with the CO_2 gas that is generated from the oxidation of the electrolyte with the oxygen released during the reduction of the $Li_{0.55}(Ni_{1/3}Co_{1/3}Mn_{1/3})O_2$ active powder.

4. Conclusion

Layered $Li_{0.45}(Ni_{0.8}Co_{0.15}Al_{0.05})O_2$ and $Li_{0.55}(Ni_{1/3}Co_{1/3}Mn_{1/3})O_2$ materials were prepared from $Li(Ni_{0.8}Co_{0.15}Al_{0.05})O_2$ and $Li(Ni_{1/3}Co_{1/3}Mn_{1/3})O$, respectively, by a chemical delithiation method using NO_2BF_4 oxidizer in an acetonitrile medium. The thermal degradation of these deintercalated powders has been studied using TGA and XRD techniques. In the case of $Li_{0.45}(Ni_{0.8}Co_{0.15}Al_{0.05})O_2$, the oxygen release from this material is associated with several structural transformations during the heat treatment, including $R\bar{3}m \rightarrow Fd3m$ (layered → unstable spinel) and $Fd3m \rightarrow Fm3m$ (unstable spine → NiO-type) transitions. However, $Li_{0.55}(Ni_{1/3}Co_{1/3}Mn_{1/3})O_2$ shows a structural transition from layered $R\bar{3}m$ phase to a more stable Fd3m spinel phase in the temperature range of 260–810 °C.

The thermal reactivity of the Layered $Li_{0.45}(Ni_{0.8}Co_{0.15}Al_{0.05})O_2$ and $Li_{0.55}(Ni_{1/3}Co_{1/3}Mn_{1/3})O_2$ powders with a non aqueous electrolytes were initially studied by a DSC technique. In both cases, the onset temperature of the reaction is exactly similar to that of the oxygen release from these materials observed by the TG analysis. $Li_{0.55}(Ni_{1/3}Co_{1/3}Mn_{1/3})O_2$ shows higher onset temperature and lower heat generation than $Li_{0.45}(Ni_{0.8}Co_{0.15}Al_{0.05})O_2$, because the oxygen release from this material takes place at higher temperature, and the amount of the oxygen released that will oxidize the electrolyte is much less compared to the case of the $Li_{0.45}(Ni_{0.8}Co_{0.15}Al_{0.05})O_2$ material.

In their present configuration, most lithium-ion batteries use non aqueous electrolytes so there is at present no means to completely suppress the oxidation of the electrolyte with charged positive electrodes unless none oxygen release type cathodes such as $LiFePO_4$ olivine are developed. Because the olivine electrode system cannot be used as it is today for high-power lithium-ion batteries applications, the $Li(Ni_{1/3}Co_{1/3}Mn_{1/3})O_2$ electrode system with its high power capabilities combined with its outstanding thermal stability could penetrate the HEV market as the first generation lithium-ion battery.

Acknowledgements

The authors acknowledge the financial support of the US Department of Energy, FreedomCAR and Vehicle Technologies Office, under Contract No. W-31-109-Eng-38.

References

[1] C.H. Chen, J. Liu, M.E. Stoll, G. Henriksen, D.R. Vissers, K. Amine, J. Power Sources 128 (2004) 278.
[2] D.P. Abraham, S.D. Poppen, A.N. Jansen, J. Liu, D.W. Dees, Electrochem. Acta 49 (2004) 4763.
[3] I. Bloom, B.W. Cole, J.J. Sohn, S.A. Jones, E.G. Polzin, V.S. Battaglia, G.L. Henriksen, J. Power Sources 101 (2001) 238.
[4] E.P. Roth, D.H. Doughty, J. Power Sources 128 (2004) 308.
[5] X. Zhang, P.N. Ross Jr., R. Kostecki, F. Kong, S. Sloop, J.B. Kerr, K. Striebel, E.J. Cairns, F. McLarnon, J. Electrochem. Soc. 148 (2001) A463.
[6] M. Balasubramanian, X. Sun, X.Q. Yang, J. McBreen, J. Power Sources 92 (2001) 1.
[7] D.P. Abraham, R.D. Twesten, M. Balasubramanian, I. Petrov, J. McBreen, K. Amine, Electrochem. Commun. 4 (2002) 620.
[8] I. Belharouak, Y.-K. Sun, J. Liu, K. Amine, J. Power Sources 123 (2003) 247.
[9] K.M. Shaju, G.V. Subba Rao, B.V.R. Chowdari, Electrochem. Acta 48 (2002) 145.
[10] S. Venkatraman, A. Manthiram, Chem. Mater. 14 (2002) 3907.
[11] S. Venkatraman, Y. Shin, A. Manthiram, Electrochem. Solid-State Lett. 6 (2003) A9.
[12] J. Rodriguez-Carvajal, Powder Diffraction Satellite Meeting of the XVth Congress of IUCr, Abstract, Toulouse, 1990, 127.
[13] M. Guilmard, L. Croguennec, D. Denux, C. Delmas, Chem. Mater. 15 (2003) 4476.
[14] M. Guilmard, L. Croguennec, C. Delmas, Chem. Mater. 15 (2003) 4484.